Image Cover Sheet

CLASSIFICATION	SYSTEM NUMBER
UNCLASSIFIED	503686

TITLE

DATA-MODEL COMPARISONS OF REVERBERATION AT THREE SHALLOW-WATER SITES

System Number:

Patron Number:

Requester:

Notes:

DSIS Use only:

Deliver to:

Data-Model Comparisons of Reverberation at Three Shallow-Water Sites

Francine Desharnais and Dale D. Ellis, *Member, IEEE*

Abstract— **Reverberation measurements made by the SACLANT Undersea Research Centre at three shallow-water sites (130–190-m depth) are compared with each other and with estimates from the DREA normal-mode reverberation model OGOPOGO. The experiments over silt-clay and sand seabeds were conducted at slightly bistatic geometries (0.7–6.0-km source-receiver separation), using explosive sources detonated at mid-water depths. The signals were received on hydrophones of either a vertical or horizontal array and analyzed in one-tenth-decade frequency bands from 25 to 1000 Hz. The data are compared with each other to investigate the site differences and frequency dependencies, and with the estimates from the reverberation model OGOPOGO to interpret the data and to obtain a qualitative measure of the scattering. For modeling purposes, geoacoustic models of the seabed were assumed, and the reverberation data were fitted by adjusting the Lambert bottom scattering coefficients. Good model agreement was obtained with both individual hydrophone and beam data. Though somewhat sensitive to the geoacoustic model, the Lambert coefficients give a measure of the frequency dependence of the scattering. For the silt-clay bottom, the scattering is weak but is independent of frequency; for the sand bottoms, the scattering is stronger and increases with frequency. These results are compared with estimates from other experiments.**

Index Terms—**Horizontal arrays, reverberation measurements, reverberation models, shallow water, vertical arrays.**

I. Introduction

RECENT years have seen renewed effort in shallow-water reverberation, both measurement and modeling. Recent conference proceedings [1]–[2] give an indication of the status of current research efforts.

The purpose of this paper is to compare and analyze broadband reverberation data collected by the SACLANT Undersea Research Centre at three shallow-water sites: one site with a silt-clay bottom and two sites with sand bottoms. The sites had relatively flat bottoms, with water depths of 130–190 m. In all cases, the sources were explosive charges detonated at approximately mid-depth and analyzed in one-tenth decade frequency bands from 25 to 1000 Hz. Data from single hydrophones and from the broadside or horizontal beams of a towed or vertical array are presented. The data are compared with each other to investigate the site differences and with estimates from the DREA normal-mode reverberation model OGOPOGO [3], [4] in order to better understand the data and to obtain a quantitative measure of the scattering.

Manuscript received June 21, 1996; revised December 23, 1996. Part of this work was performed while the authors were on exhange with the SACLANT Undersea Research Centre, La Spezia, Italy.

The authors are with the Defence Research Establishment Atlantic, Dartmouth, Nova Scotia, B2Y 3Z7 Canada.

Publisher Item Identifier S 0364-9059(97)03405-5.

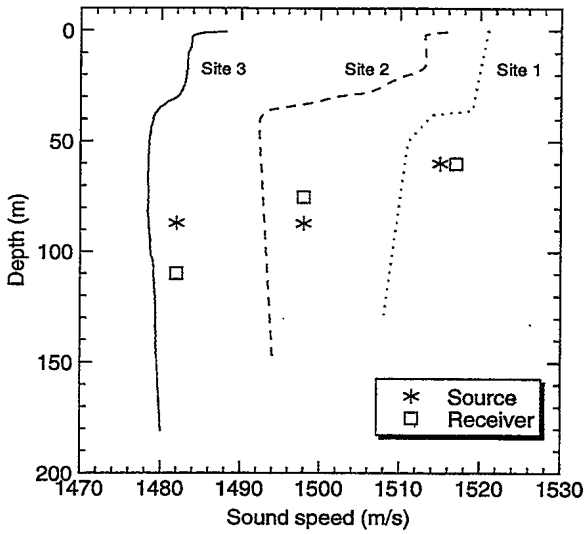

Fig. 1. Representative sound-speed profiles for Site 1 (dotted line), Site 2 (dashed line), and Site 3 (solid line). The star indicates the source depth and the square the receiver depth for each site.

For modeling purposes, a geoacoustic model of the seabed was assumed, and the reverberation data were fitted by adjusting the Lambert bottom scattering coefficients. The geoacoustic model gives the sound speed, density, and attenuation in the seabed as a function of depth and is a key factor in determining the acoustic propagation. Though somewhat sensitive to the assumed geoacoustic model, the Lambert coefficients give a measure of the frequency dependence of the scattering. Over the silt-clay bottom, the scattering is independent of frequency and relatively weak; over the two sand bottoms, the scattering is stronger and increases with frequency.

II. Description of the Experiments and Data

The sites were chosen to have relatively flat bathymetry to enable interpretation of the data and facilitate comparison with a range-independent reverberation model. The three sites and experiments are briefly described in this section.

A. Site 1

The average water depth at Site 1 is 130 m over a silt-clay bottom. The sound-speed profile was downward refracting (Fig. 1), and the winds were light throughout the experiment.

One-kg explosive charges were used for the reverberation experiment, with a detonation depth of 60 m. The receiver

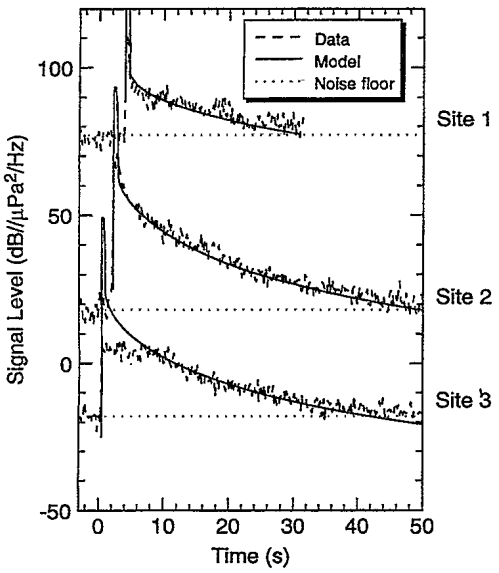

Fig. 2. Reverberation data and model estimates for the 316-Hz band at the three sites. The dashed lines are the data, the solid lines are the model estimates, and the dotted lines are the noise floor. The scale on the right applies for Site 1; Sites 2 and 3 are offset by −50 and −100 dB, respectively.

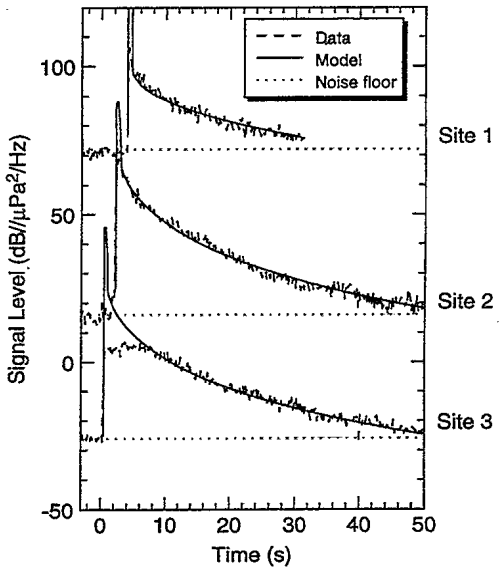

Fig. 3. Reverberation data and model estimates for the 631-Hz band at the three sites. See caption of Fig. 2 for explanation of the curves.

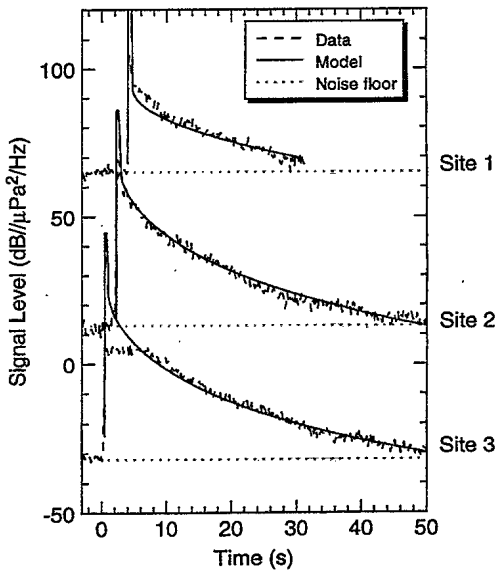

Fig. 4. Reverberation data and model estimates for the 1000-Hz band at the three sites. See caption of Fig. 2 for explanation of the curves.

was a horizontal array of 64 hydrophones at 1-m spacing, towed at a nominal depth of 60 m. Signals from the 64 hydrophones were processed through a time-domain beam former, producing 65 beams equally spaced in the cosine of the steering angle from forward endfire to aft endfire. A Hann[1] spatial window with 64 nonzero weights was used to form the beams. The time series for the beams and hydrophones were sampled at 3000 Hz and analyzed in one-tenth decade (almost equivalent to one-third octave) frequency bands from 25 to 1000 Hz using 512-point FFT's, giving reverberation estimates for each band at 0.17-s intervals.

Fig. 2 (upper dashed line) shows the reverberation level as a function of time for a charge 6 km distant from an omnidirectional hydrophone located in the middle of the towed array, for the frequency band centered at 316 Hz. The instant of the detonation is at zero time, the main blast arrives at 4 s, is clipped for about 1 s, and decays rapidly. After about 30 s, there are returns from islands and bathymetric features so the data are not shown. The dotted line immediately below the upper dashed line represents the ambient noise floor for the 316-Hz frequency band. The other curves on the figure are from other sites (dashed lines) and from model estimates (solid lines) and will be discussed later.

Figs. 3 and 4 (upper dashed lines) show data from the same charge, for the 631- and 1000-Hz frequency bands, respectively. Note that as the frequency increases, the reverberation-to-noise level increases at short times (due to the decrease in the ambient noise background).

B. Site 2

The average water depth at Site 2 is 150 m over a sand bottom. The bottom is characterized by long parallel ridges spaced by 10 km on average. The average peak to trough height is about 20 m corresponding to an average slope of about 0.2°; peak to troughs as high as 50 m (0.5°) were measured and local slopes would be higher than the average. The sound-speed profile had a downward refracting layer near the surface and a weak mid-channel duct (Fig. 1). The winds were approximately 15 knots during the experiments.

The receiver, in this case a vertical array since the towed array was not deployed, was moored in a trough between two ridges, and the sources (0.8-kg explosive charges) were dropped along the same trough. The charge used for the data presented in this paper was detonated 3.3 km from the array at a depth of 87 m. The signals from 32 hydrophones were recorded; the separation between the hydrophones was 1 m, and the acoustic center was at 75-m depth. The 32 signals were

[1] The square cosine window is named after the Austrian meteorologist Julius Van Hann; it is often erroneously called a *hanning* window [5]

processed through a time-domain beam former, producing 33 beams spaced equally in cosine of the steering angle from upward endfire to downward endfire. A square spatial window was used to form the beams. The data were analyzed in one-tenth decade frequency bands, as described for Site 1.

Fig. 2 (middle dashed line) shows the reverberation level from one charge as a function of time for an omnidirectional hydrophone located in the middle of the vertical array, for a frequency of 316 Hz. The direct blast arrives at 2.2 s and is briefly overloaded. The dotted line immediately below indicates the noise floor. The middle curve is offset by −50 dB relative to the upper curve. Figs. 3 and 4 (middle dashed lines) show the same data for frequency bands centered at 631 and 1000 Hz, respectively (also offset −50 dB).

C. Site 3

The water depth at Site 3 is 190 m, and the sand bottom is reasonably flat in the area. The sound-speed profile also displayed the mixed surface layer over a weak midwater column duct, as shown in Fig. 1. The winds averaged 12 knots with a sea state of 3.

The sources were 0.8-kg explosive charges detonated at 87-m depth. The charges were detonated approximately 650 m from the receiver, a horizontal array towed at a depth of 110 m. The separation between the hydrophones was either 2 m (frequencies below 400 Hz) or 0.5 m (above 400 Hz). For each frequency, 64 signals were processed through a time-domain beam former, producing 65 beams spaced equally in cosine of the steering angle from forward endfire to aft endfire. A Hann spatial window with 64 nonzero weights was used. The data were analyzed in one-tenth-decade frequency bands from 50 to 1250 Hz.

Fig. 2 (lower dashed line) shows the reverberation level as a function of time received on an omnidirectional hydrophone located in the middle of the towed array, for the 316-Hz band. The direct blast arrives less than 0.5 s after the detonation and overloads the system for about 4 s. The dotted line represents the noise floor. The curves are offset by −100 dB relative to the upper curve. Figs. 3 and 4 (lower dashed lines) show the same data for frequency bands of 631 and 1000 Hz, respectively (also offset −100 dB).

D. Comparison of Data at Three Sites

Figs. 2–4 allow for interesting comparisons of the three sites over a range of frequencies.

The distance between the source and receiver was different for each site, therefore, the peaks corresponding to the direct arrivals are not aligned. However, choosing the instant of detonation as time zero, rather than the instant of reception of the direct arrival, allows reverberation from different bistatic separations to be compared with each other and with monostatic results; this is because, as time increases, the equal-time ellipses for bistatic geometries rapidly approach circles centered at the mid-point between the source and receiver. Measurements by Urick [6] and calculations by Ellis [4] illustrate how the bistatic effects disappear very quickly after the main arrival.

Because the source–receiver distance was relatively short at Site 3, the hydrophones were overloaded and the data were clipped for approximately 4 s. This results from the multiple surface-bottom reflections (fathometer returns) and nearby steep-angle scattering. Some clipping also occurred at Sites 1 and 2 but for shorter duration (less than 1 s).

The slope of the reverberation curves (or rate of decay) depends mainly on the rate of propagation loss with range which is affected by the bottom composition. A soft absorbing bottom causes high propagation losses, and the reverberation levels will decrease more quickly in time. This is particularly effective at high frequency, because the high-order modes get stripped off at short ranges, leading to even higher rates of decay of the levels. However, the scattering strength of the boundaries (ocean surface and bottom) and ocean body (volume reverberation) will also have an effect on the overall reverberation levels. The resulting curve is a delicate balance between the two effects.

The slope of the reverberation curves is increasingly steeper from Site 2 to Site 3 to Site 1, which suggests that the sand bottoms of Site 2 and 3 are softer (have more loss) than the clay-silt bottom of Site 1. However, the reverberation levels at Site 1 are lower than the levels of Sites 2 and 3 (with Site 3 displaying the highest levels). This is partly due to the intrinsic scattering strengths; for a given incident angle, higher bottom scattering is expected from a sand bottom than from a clay bottom, since the sand bottom is likely to be rougher and support more features.

Because the sound-speed profiles are downward refracting at all three sites, bottom reverberation dominates surface reverberation, even at Sites 2 and 3 where the surface winds were strong. This was confirmed by the model calculations which will be discussed in the next section.

Note that the reverberation-to-noise ratio decreases as the frequency decreases. At frequencies below 300 Hz, the ambient noise from shipping and other activities can be quite high. This was particularly evident at Sites 1 and 3.

III. Model-Data Comparisons

To help interpret the results, the data were compared with estimates from a shallow-water reverberation model. The bistatic normal-mode reverberation model OGOPOGO is described by Ellis [3], [4], and is an extension of the method of Bucker and Morris [7]. The propagation is described in terms of normal modes; the specific normal-mode compute engine is the DREA normal-mode model PROLOS [8]. The travel times of the reverberation signals are derived from the modal group velocities. Both monostatic and bistatic geometries can be handled, as well as horizontal or vertical arrays for source and receiver. Volume reverberation from the water column or the subbottom is not currently included in the model, but surface and bottom scattering are calculated. The scattering is assumed to occur at the ocean surface or water–sediment interface and is determined by empirical scattering functions and ray-mode analogies. The environmental inputs required by the model include: the sound-speed profile in the water, the geoacoustic model for the seabed (a series of isovelocity layers), the

TABLE I
GEOACOUSTIC MODELS FOR THE THREE SITES

	layer thickness (m)	compressional sound speed (m/s)	density (g/cm^3)	attenuation (dB/m-kHz)
Site 1	half-space	1600.	1.8	0.09
Site 2	0.33	1525.	1.6	0.33
	0.34	1550.	1.6	0.33
	0.33	1575.	1.6	0.33
	1.00	1600.	1.7	0.33
	1.00	1700.	1.7	0.33
	half-space	1750.	1.8	0.2
Site 3	0.33	1525.	1.6	0.33
	0.34	1550.	1.6	0.33
	0.33	1575.	1.6	0.33
	half-space	1600.	1.8	0.33

source–receiver separation, source and receiver depths and beam patterns, and parameters describing the surface and bottom scattering functions. The output is reverberation signal level as a function of time for any selected beam of a horizontal or vertical array, or for an omnidirectional receiver.

The surface scattering is based on the Chapman–Harris empirical model [9], which relates the surface scattering strength to wind speed. Because the sound-speed profiles are downward refracting at all three sites, bottom reverberation dominates over surface reverberation. At Site 1, surface reverberation was negligible and was not included in the calculations. At Site 2, the winds were 15 knots, but calculations showed surface reverberation to be minimal; this is likely due to the strongly downward refracting sound-speed profile (Fig. 1). At Site 3, some surface reverberation was present in the data; the modeling used a wind speed of 12 knots.

The scattering from the bottom follows the Mackenzie–Lambert rule [10]

$$B(\theta, \phi) = \mu \sin\theta \sin\phi \tag{1}$$

where θ and ϕ are the incident and scattered grazing angles, and μ is a proportionality constant. We refer to $10 \log \mu$ as the Lambert coefficient (in dB). The Lambert coefficient is directly related to the overall scattering strength at the site, and a value of -27 dB is regularly used in the literature, independent of frequency. We use it as an adjustable parameter to help characterize the sites and frequency dependence.

The Lambert coefficient can be estimated for any given frequency band by data-model comparisons. A good geoacoustic model is required for the bottom. If propagation loss data are available, they can be used to refine the bottom model by data-model comparisons. The reverberation model is run with an initial guess at the Lambert coefficient. If the bottom model is adequate, the time decay rate of the modeled reverberation level will match that of the reverberation data (whether it is a beam time series or an omnidirectional receiver time series), although the levels might be offset by a constant level. The offset is added to the initial estimate of the Lambert coefficient, and the reverberation model is rerun with the updated value. The level offset can differ for various frequency bands, which leads to a frequency-dependent Lambert coefficient.

The geoacoustic models assumed for our calculations are listed in Table I. The soft bottom at Site 1 consists of clay mixed with some sand and silt. A simplification of Jensen's geoacoustic model for the area [11] is included in Table I; the original model, based on propagation loss model-data comparisons, had a thin (2 m) softer layer above the half-space, with a sound speed as low as 1520 m/s near the surface.

The bottom information for Site 3 was derived from the analysis of bottom cores, combined with propagation loss model-data comparisons [12]. A simplified geoacoustic model for the site is included in Table I. Although the top sediment is believed to be sand, the addition of a low-speed surface layer 1 m thick (split into three layers to simulate a surface gradient) was necessary to fit the high-frequency propagation and reverberation data.

A sand bottom with long parallel ridges characterizes Site 2. The geoacoustic model shown in Table I was used for the modeling. The parameters for the deeper layers are close to the description from Max [13] and properties determined by Ellis and Chapman [14] for a similar area, but the low-speed surface layer of Site 3 was also added at this site to better fit the high-frequency data. We do not have any direct evidence for this gradient, but a sand bottom often has a steep sound-speed gradient near the water–sediment interface. We are simulating this with a few isovelocity layers.

A. Comparison with Hydrophone Data

The reverberation levels as a function of time were modeled with OGOPOGO for all three sites and several frequency bands between 50 and 1000 Hz, for an omnidirectional receiver. For Site 1 the average source spectral levels (dB re $1\mu Pa^2$-s at 1 m) were obtained by scaling measurements from a 0.45-kg charge; the levels are shown in Table II. For Sites 2 and 3, the average levels for the SUS charges were obtained from measurements at SACLANTCEN; the levels are also in Table II. The OGOPOGO model assumes a CW type of pulse of constant intensity; a 0.5-s duration pulse with source level 3 dB higher than the spectral levels indicated was used to give the correct energy.

The results are shown in Figs. 2–4 for frequencies of 316, 631, and 1000 Hz, respectively. The Lambert coefficients

TABLE II
SOURCE LEVELS (dB re 1μ Pa^2-s at 1 m) AS A FUNCTION OF FREQUENCY FOR THE THREE SITES

Frequency (Hz)	50	316	398	501	631	794	1000
Site 1	—	198.8	198.5	196.4	196.3	195.5	192.8
Site 2,3	207.8	199.1	197.7	196.4	195.3	194.2	193.2

TABLE III
LAMBERT COEFFICIENTS AS A FUNCTION OF FREQUENCY FOR THE THREE SITES

Frequency (Hz)	Lambert coefficient (dB)		
	Site 1	Site 2	Site 3
50	–		-20
158	–	-33	-20
316	-35	-28	-17
398	-36	-23	–
501	-35	-21	–
631	-35	-16	-12
794	-36	-14	-12
1000	-36	-14	-11

leading to the best data-model fits are listed in Table III. The model results fit the data reasonably well, especially at low frequency. Above 800 Hz, the rate of decay of the modeled curves is consistently too low for all sites, although the biggest discrepancy between data and model is found at Site 1. A steeper slope could be achieved for all sites with a softer, more absorbing surface layer. At Site 1, the geoacoustic model is harder in the first 2 m than given by Jensen [11]. Ellis and Gerstoft [15] used inversion techniques with a gradient model for the sediments to obtain better fits to the data. Nonetheless, the modeling results presented here are satisfactory, and the derived Lambert coefficients are quite similar to those of Ellis and Gerstoft.

B. Comparison with Beam Data

Additional calculations were made to test the ability of OGOPOGO to estimate beam data and compare with data and model estimates from an omnidirectional sensor. Except for the beam patterns, the same inputs were used for both the beam and single-hydrophone calculations. The dashed lines in Figs. 5–7 show the reverberation data for Sites 1, 2, and 3, respectively; the solid lines are the modeling results; the dotted lines represent the noise floor.

Fig. 5 shows data and model estimates for an omnidirectional hydrophone and the broadside beam of the horizontal array at Site 1 for the 501-Hz band. Fig. 6 shows data and model estimates for an omnidirectional hydrophone and the broadside beam of the vertical array at Site 2 for the 501-Hz band. At Site 3, analyzed data were not available in the 501-Hz band, so results from the next higher band (631 Hz) are shown in Fig. 7 for a hydrophone and the broadside beam of the towed array.

The model agrees reasonably well with the data in all cases, whether the data come from an omnidirectional sensor, a horizontal array broadside beam, or a vertical array broadside beam. In the case of the horizontal array, the Lambert coefficient leading to the best fit for the omnidirectional receiver slightly overestimates the predicted levels for the broadside beam. We do not have a good explanation of this, except perhaps spatial variability; the side lobes of the beams do not contribute significantly in the model calculations and are set at a reasonable level (−35 dB). The broadside vertical beam underestimates the measured reverberation; we suspect that this is due to array tilt, which would point the array beam pattern at the bottom, increasing the measured reverberation.

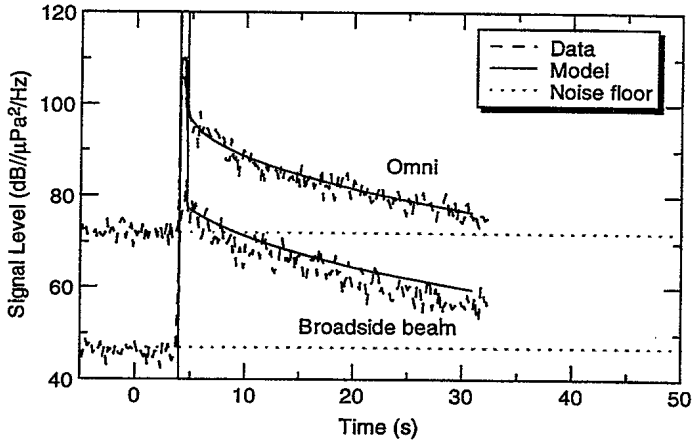

Fig. 5. Reverberation level as a function of time at Site 1 for an omnidirectional receiver (upper curves) and the horizontal array broadside beam (lower curves) at 501 Hz. The dashed lines are the data, the solid lines are the model estimates, and the dotted lines are the noise floor. The Lambert coefficient is −35 dB.

IV. DISCUSSION

Fig. 8 summarizes the reverberation modeling results by plotting the derived Lambert coefficients from Table III as a function of frequency for Site 1 (squares), Site 2 (triangles), and Site 3 (diamonds). The Site 1 coefficients for the silt-clay bottom are independent of frequency and are 5–10 dB lower than Mackenzie's generic value of −27 dB, indicating low

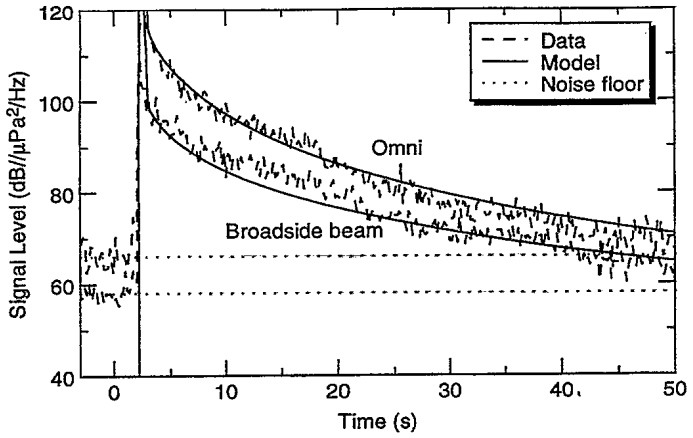

Fig. 6. Reverberation level as a function of time at Site 2 for an omnidirectional receiver (upper curves) and the vertical array broadside beam (lower curves) at 501 Hz. The dashed lines are the data, the solid lines are the model estimates, and the dotted lines are the noise floor. The Lambert coefficient is −19 dB.

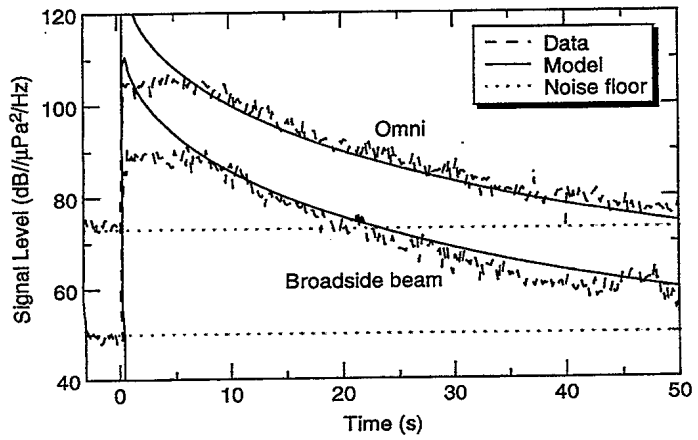

Fig. 7. Reverberation level as a function of time at Site 3 for an omnidirectional receiver (upper curves) and the horizontal array broadside beam (lower curves) at 630 Hz. The dashed lines are the data, the solid lines are the model estimates, and the dotted lines are the noise floor. The Lambert coefficient is −13 dB.

bottom scattering in the area. The low-frequency coefficients of Site 2 are similar in magnitude. Above 300 Hz, however, the Lambert coefficients for the sandy bottom at Sites 2 and 3 are much higher than this. The dashed line in Fig. 8 represents a linear fit to the Site 3 coefficients above 150 Hz; it shows a frequency dependence of 3.55 dB/octave (or $f^{1.18}$, where f is the frequency). The data from Site 2, fitted with the dotted line, have a steeper frequency dependence ($f^{2.66}$).

A frequency dependence similar to that of the Site 3 data is found in literature for sand bottoms [16]–[18]. In the 0.8–4.0-kHz region, Zhou *et al.* [19] show frequency dependencies ranging from $f^{0.8}$ to $f^{2.8}$ for a range of bottom types ranging from fine sand to silty sand and sandy silt. The increase in scattering in [16] follows the 1.1 power of frequency (3.3 dB/octave) for data from the North American Continental Rise and from the Bermuda Rise (frequencies above 400 Hz). Excluding the 50-Hz coefficient, our data show a similar

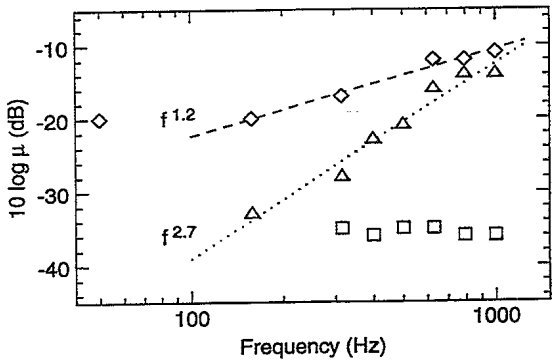

Fig. 8. Lambert coefficient as a function of frequency for Site 1 (squares), Site 2 (triangles), and Site 3 (diamonds). The lines represent linear fits to the points for Sites 2 and 3 at frequencies above 150 Hz.

increase of the Lambert coefficient to the 1.18 power of frequency. Urick's [6] shallow-water data show a 2-dB/octave, or $f^{0.9}$ dependence. Thiele and Tielbürger [18] offer the following experimental relationship for the Lambert coefficient as a function of frequency for sand bottoms at several sites:

$$10\log\mu = \begin{cases} a, & \text{if } f \geq f_0 \\ a + b\log(f/f_0), & \text{if } f < f_0 \end{cases} \qquad (2)$$

with f_0 typically between 2 and 4 kHz, a is less than −15 dB and $b \approx 18$ (equivalent to a power law of $f^{1.8}$). The Lambert coefficients from Table III are higher than those given in [18]; however, they fit a similar equation. Note that the parameter f_0 denotes a plateau, above which the Lambert coefficient does not increase. The parameter f_0 cannot be determined since we have no high-frequency data; however, it would be greater than our highest frequency of 1 kHz for both Sites 2 and 3. If we assume $f_0 = 1$ kHz, the resultant values for Site 2 are $a = -12.6$ and $b = 26.6$; for Site 3, $a = -10.6$ and $b = 11.8$.

Thiele [20] and Cable *et al.* [21] indicate there may be a minimum in scattering in the 100–500-Hz frequency band. Our data in the lower part of this regime were ambient noise-limited. However, the point at 50 Hz for Site 3, which was excluded from our fit, falls above the straight line.

The high bottom-scattering coefficients at the higher frequencies were obtained including bottom and surface reverberation in the calculations. However, volume reverberation in the water column, or possibly the sediments, could be a contributing factor and is not included in the model calculations. Thiele and Tielbürger [18] have noted volume reverberation from fish schools can be significant. Weston [22], [23] has noted that fish can cause significant transmission loss and reverberation effects. Also, Akal *et al.* [24] and other investigators have noted that volume reverberation due to resonant scattering from fish bladders can increase rapidly above a few hundred hertz. There was considerable fishing activity at Site 2 during the period of the experiments.

Volume reverberation due to internal waves is another potential explanation for the high bottom-scattering coefficients at higher frequencies. Although the oceanographic parameters were not monitored closely enough during these

three experiments to confirm the presence of such waves, the variability in the thermocline depth of the various sound-speed profiles suggest that internal waves may have been present at Sites 2 and 3, but likely not at Site 1. As demonstrated by Zhou and Zhang [25], internal waves can induce a clear frequency dependence in the propagation loss, but the effect will vary with the wave (packet) pattern. The right oceanic conditions might have influenced the frequency dependence seen in the reverberation data.

The frequency dependence of the derived backscattering strengths can be biased by systematic errors in any of the inputs, or inadequacies of the model itself. However, we expect it is the uncertainties in the transmission loss (resulting from the geo-acoustic inputs for the bottom) which are the major cause of any uncertainty. Where it is available, such as at Site 3, propagation data as well as reverberation data can be used to improve the inputs.

Another approach is to simultaneously fit the geoacoustic model and scattering parameters. Ellis and Gerstoft [15] have used inversion techniques to simultaneously extract bottom sound speed and scattering strengths at Site 1. Their multifrequency results, using a sound-speed gradient in the bottom, produced frequency-independent scattering strength similar in magnitude to the results here for a 1600-m/s half space.

V. Conclusion

Low-frequency reverberation measurements from three shallow-water sites have been presented and compared with estimates from a reverberation model utilizing normal mode sound propagation. The measurements add to the body of knowledge about reverberation in shallow water. Bottom reverberation dominated at all three sites, though surface reverberation contributed at high frequencies at one site.

The OGOPOGO model with a geoacoustic model and adjustable bottom Lambert scattering coefficient provides a good fit to the data over a broad frequency band and different sites. The beam pattern modeling approach seems to be in reasonable agreement with the data, providing evidence to validate this approach in reverberation modeling.

The calculations indicate there is a strong coupling between transmission loss and reverberation, and a good geoacoustic model is required to fit both types of data. However, a simple bottom description was enough in the two cases presented here to achieve good model-data agreement.

Based on the model-data fits, estimates of the frequency dependence of the bottom scattering strengths were obtained. Of the three data sets, the silt-clay bottom has low scattering coefficients with no frequency dependence. The two sand-bottom sites displayed a strong frequency dependence and high scattering coefficients at frequencies above 600 Hz. The frequency dependence is consistent with measurements by other investigators in shallow water at these frequencies. Over the sand bottoms, the derived scattering strengths at high frequencies are higher than those observed by other investigators; effects of volume reverberation cannot be ruled out.

Acknowledgment

The data presented in this paper were collected during three separate sea trials conducted by the Applied Acoustics Group (Project 05) at the SACLANT Undersea Research Centre, La Spezia, Italy.

References

[1] D. D. Ellis, J. R. Preston, and H. G. Urban, Eds., *Ocean Reverberation*. Dordrecht, The Netherlands: Kluwer, 1993.
[2] "Underwater acoustic scattering," in *Proc. Inst. Acoust.*, vol. 16, pt. 6, 1994.
[3] D. D. Ellis, "A shallow-water normal-mode reverberation model," *J. Acoust. Soc. Amer.*, vol. 97, pp. 2804–2814, 1995.
[4] ———, "Shallow water reverberation: Normal-mode model predictions compared with bistatic towed-array measurements," *IEEE J. Oceanic Eng.*, vol. 18, pp. 474–482, 1993.
[5] S. L. Marple, *Digital Spectral Analysis with Applications*. Englewood Cliffs, NJ: Prentice-Hall, 1987, p. 139.
[6] R. J. Urick, "Reverberation-derived scattering strength of the shallow sea bed," *J. Acoust. Soc. Amer.*, vol. 68, pp. 392–397, 1970.
[7] H. P. Bucker and H. E. Morris, "Normal-mode reverberation in channels or ducts," *J. Acoust. Soc. Amer.*, vol. 44, pp. 827–828, 1968.
[8] D. D. Ellis, "A two-ended shooting technique for calculating normal modes in underwater acoustic propagation," DREA Rep. 85/105, Sept. 1985.
[9] R. P. Chapman and J. H. Harris, "Surface backscattering strengths measured using explosive sound sources," *J. Acoust. Soc. Amer.*, vol. 34, no. 10, pp. 1592–1597, 1962.
[10] K. V. Mackenzie, "Bottom reverberation for 530- and 1030-cps sound in deep water," *J. Acoust. Soc. Amer.*, vol. 33, pp. 1948–1504, 1961.
[11] F. B. Jensen, "Comparison of transmission loss data for different shallow water areas with theoretical results provided by a three-fluid normal-mode propagation model," in *Sound Propagation in Shallow Water, SACLANTCEN Conf. Proc. CP-14*, O. F. Hastrup and O. V. Olesen, Eds., Nov. 1974, pp. 79–92.
[12] T. Akal and F. Desharnais, personal communication, 1995.
[13] M. D. Max, E. Michelozzi, F. Turgutcan, and B. Tonarelli, "Geoenvironmental characterization of selected shallow-water sites on the western European continental shelf (SWAP)," SACLANTCEN SM-288, SACLANT Undersea Research Centre, La Spezia, Italy, 1995.
[14] D. D. Ellis and D. M. F. Chapman, "Modeling of shear-wave related acoustic propagation on the U.K. Continental Shelf," DREA Tech. Memo. 84/P, Sept. 1984.
[15] D. D. Ellis and P. Gerstoft, "Using inversion techniques to extract bottom scattering strengths and sound speeds from shallow-water reverberation data," in *Proc. 3rd Eur. Conf. Underwater Acoustics*, J. S. Papadakis, Ed., FORTH Heraklion, Crete, Greece, 1996, pp. 557–562.
[16] H. M. Merklinger, "Bottom reverberation measured with explosive charges fired deep in the ocean," *J. Acoust. Soc. Amer.*, vol. 44, pp. 508–513, 1968.
[17] C. M. McKinney and C. D. Anderson, "Measurements of backscattering of sound from the ocean bottom," *J. Acoust. S. Amer.*, vol. 36, pp. 158–163, 1964.
[18] R. Thiele and D. Tielbürger, private communication, 1992.
[19] J. X. Zhou, D. H. Guan, E. C. Shang, and E. S. Luo, "Long-range reverberation and bottom scattering strength in shallow water," *Chinese J. Acoust.*, vol. 1, pp. 54–63, 1982.
[20] R. Thiele, "Measured dependence of transmission loss and reverberation from the sea bottom at the Fladengound experiment," in *Acoustics and the Sea-bed*, N. G. Pace, Ed. Bath, U.K.: Bath Univ. Press, 1983, pp. 207–213.
[21] P. Cable, J. O'Connor, and M. Steele, "Shallow water bottom scattering strength at low frequencies," in *Underwater Acoustic Scattering, Proc. Inst. Acoustics*, 1994, vol. 16, pt. 6, pp. 209–216.
[22] P. A. Ching and D. E. Weston, "Wideband studies of shallow water acoustic attenuation due to fish," *J. Sound Vib.*, vol. 18, pp. 499–510, 1971.
[23] D. E. Weston and P. D. Hocking, "Interference patterns in shallow-water reverberation," *J. Acoust. Soc. Amer.*, vol. 87, pp. 639–651, 1990.
[24] T. Akal, R. K. Dullea, G. Guidi, and J. H. Stockhausen, "Low-frequency volume reverberation measurements," *J. Acoust. Soc. Amer.*, vol. 93, pp. 2535–2548, 1993.
[25] J. X. Zhou and X. Z. Zhang, "Resonant interaction of sound wave with internal solitons in the coastal zone," *J. Acoust. Soc. Amer.*, vol. 90, pp. 2042–2054, 1991.

Francine Desharnais was born in Cap-de-la-Madeleine, Quebec, Canada, in 1964. She received the B.Sc. degree in physics and the M.Sc. degree in meteorology from the Université du Québec à Montréal, Quebec, Canada, in 1986 and 1988, respectively.

From 1988 to 1991, she worked with the Applied Acoustics Group at the Defence Research Establishment Atlantic, Dartmouth, Nova Scotia, Canada, and since 1996 she has been with the Ocean Acoustics Group. From 1992 to 1995, she was a member of the Large Scale Acoustics and Oceanography Group at the SACLANT Undersea Research Centre, La Spezia, Italy. Her current research interests are in the modeling and data interpretation of underwater noise and reverberation. She is an Associate Editor of *Canadian Acoustics*.

Ms. Desharnais is a member of the Canadian Acoustical Association and the Acoustical Society of America.

Dale D. Ellis (M'92) was born in Bathurst, New Brunswick, Canada, in 1949. He received the B.Sc. degree in mathematics and physics from Mount Allison University, Sackville, NB, in 1970 and the M.Sc. and Ph.D. degrees in theoretical nuclear physics from McMaster University, Hamilton, Ontario, Canada, in 1971 and 1976, respectively.

Since 1977, he has been employed at Defence Research Establishment Atlantic in Dartmouth, Nova Scotia, Canada, and is currently Leader of the Modeling and Systems Analysis Group. From 1990 to 1994, he was a Scientist at the SACLANT Undersea Research Centre in Italy. His main research efforts have been in numerical modeling of shallow-water propagation and scattering and comparisons with data. His current emphasis is on rapid environmental assessment.

Dr. Ellis is a fellow of the Acoustical Society of America and a member of the Canadian Acoustical Association, the Canadian Applied Mathematics Society, and the Royal Astronomical Society of Canada.